ISSN 0031-918X, The Physics of Metals and Metallography, 2014, Vol. 115, No. 10, pp. 1017–1022. © Pleiades Publishing, Ltd., 2014.
Original Russian Text © V.L. Arbuzov, S.E. Danilov, V.A. Kazantsev, V.V. Sagaradze, 2014, published in Fizika Metallov i Metallovedenie, 2014, Vol. 115, No. 10, pp. 1080–1085.

STRENGTH AND PLASTICITY

Radiation-Induced Strengthening of Al- and Ti-Modified Fe–Ni Alloys during Electron Irradiation

V. L. Arbuzov, S. E. Danilov, V. A. Kazantsev, and V. V. Sagaradze

Institute of Metal Physics, Ural Branch, Russian Academy of Sciences, ul. S. Kovalevskoi 18, Ekaterinburg, 620990 Russia

e-mail: danilov@imp.uran.ru

Received December 14, 2013; in final form, March 26, 2014

Abstract—A complex study of Fe–Ni, Fe–Ni–Ti, and Fe–Ni–Al alloys irradiated by electrons with an energy of 5 MeV at a temperature of 423 K has been carried out. The relationship between radiation-induced strengthening, radiation-induced defects, and radiation-induced structural and phase transformations has been considered. In the Fe–Ni alloy, vacancy clusters play a leading role in radiation-induced strengthening; in the Fe–Ni–Ti and Fe–Ni–Al alloys, in addition to the vacancy clusters, the evolution of secondary-phase precipitates and the relief of solid-solution hardening are of great significance.

Keywords: iron–nickel alloys, titanium, aluminum, irradiation, electrons, strengthening, radiation-induced defects, vacancy clusters, precipitates, intermetallic compounds, phase transformations

DOI: 10.1134/S0031918X14100032

INTRODUCTION

The knowledge of mechanisms of radiation-induced damage and radiation stability is a necessary condition for the development of new promising structural materials for nuclear reactors. Changes in mechanical characteristics of materials due to irradiation are primarily related to the evolution of their microstructure. Depending on the type and energy of the ionizing radiation, radiation-induced damages appear either as clusters of interstitial or vacancy defects, which are formed during the passage through cascades of atomic displacements and their evolution, or as single movable point defects [1]. Freely migrating defects can substantially accelerate processes of the transformation of the microstructure in real materials (that is most frequently metastable), which tend to bring these materials into an equilibrium state. Competing processes that lead to the appearance of nonequilibrium states due to the retention of a system in a nonequilibrium state during irradiation can also be stimulated. The main nonequilibrium processes are processes of the formation of defect clusters and segregates of elements up to the appearance of precipitates. These segregates can be homogeneous, but most frequently they appear on clusters of point defects, dislocations, grain boundaries, and interfaces [2, 3]. In many cases, the irradiation of metals leads to their radiation-induced strengthening due to the formation of a specific defect structure (which consists of clusters and complexes of defects), vacancy pores, dislocation loops, etc. [2, 3]. In steels and alloys, changes in mechanical properties can result from additional factors, namely, structural and phase transformations. Radiation-induced structural and phase transformations (the phase separation of solid solutions [4, 5] and precipitation hardening [6] during irradiation) require a comprehensive study with account for the interaction of point defects with impurities and alloying elements using model systems to develop a new generation of materials for nuclear power engineering.

The amount and sizes of precipitates of new phases that are formed during the aging and irradiation of stainless steels and alloys affect many macroscopic characteristics of these materials. This concerns the mechanical characteristics and the susceptibility to vacancy swelling [7]. Phase formation under irradiation substantially depends on a number of factors, such as, the type of radiation, the exposure dose, and the irradiation temperature [2, 3, 7].

Invar Fe–Ni alloys possess unique magnetomechanical properties. They are promising structural materials for nuclear power engineering and are used as model materials to study the behavior of austenitic stainless steels under various external effects. The investigation of these alloys can be helpful in understanding processes that occur in more complex systems. The as-quenched Fe–Ni–Ti and Fe–Ni–Al alloys are supersaturated solid solutions; in the course of the aging of these alloys, an ordered γ' phase precipitates, the composition of which is close to Ni_3Ti or Ni_3Al [8, 9]. These phases have a lattice parameter close to that of the matrix and are coherently bound with it.

The aim of this work was to carry out a complex study of processes of the radiation-induced aging of the Fe–Ni, Fe–Ni–Ti, and Fe–Ni–Al alloys, as well as of specific features of structural and phase transformations occurred and changes in the mechanical characteristics of the alloys. The alloys were irradiated at 423 K using electron radiation, which generated freely migrating point defects.

EXPERIMENTAL

The objects of the study were the model alloys Fe–34.7 at % Ni (Fe–Ni), Fe–34 at % Ni–3 at % Ti (Fe–Ni–Ti), and Fe–31.2 at % Ni–10.8 at % Al (Fe–Ni–Al) prepared by vacuum melting using pure components. Specimens of the alloys were rolled, drawn, and cut; after that, they were electrolytically polished, annealed in pure helium for 1 h at 1473 K, and quenched in water at a rate of 1000 K/s. The X-ray diffraction (XRD) data show that all the alloys are in a single-phase perfectly austenitic state.

The XRD structural analysis of the quenched specimens was carried out using a DRON-2 diffractometer. Measurements of the residual electric resistivity, dilatometry, and electron microscopy were also used. The mechanical characteristics of the specimens were determined.

The mechanical characteristics and the electric resistivity were measured using wires ~0.2 mm in diameter. The mechanical tests were carried out using an FP-100 testing machine at room temperature and a strain rate of 1.5×10^{-3} s^{-1}. The yield stress, the ultimate strength, and the relative elongation were calculated using the stress–strain curve taking into account the geometric dimensions of the specimens. The residual electric resistivity was measured using the standard potentiometric method with a measurement error of 0.02%.

Dilatometry was performed using a DL-1500 RHP dilatometer in the dynamic mode in the range of room temperature to 373 K with a constant rate of heating of 2 K/min in pure helium. The specimens for measurements were plates ~0.15 mm thick.

The electron-microscopic examinations were carried out using a JEM-200 CX electron microscope at an accelerating voltage of 160 kV. The specimens were shaped as thin foils. Particles of the second phase were identified using the dark-field procedure.

The Fe–Ni–Ti alloy was additionally studied using scanning tunnel microscopy (STM). At the initial stages of the formation of the new phase, when precipitates are not greater than a few nanometers in size, the coherency and dispersity of the precipitates make it difficult to examine them using standard methods (electron microscopy or XRD). STM allows one to examine nanosized objects. The capabilities of STM in the case under consideration and the procedure of measurements were described in our previous work [10]. The examinations were carried out using an STM-U1 scanning tunnel microscope. After each stage of annealing or irradiation, the specimens were electrolytically etched to a depth of a few microns to remove surface contaminations and to reveal the microstructure. To obtain a detailed information on the state of each specimen, ten or more images of various portions of its surface were taken. The alloys were irradiated by electrons with an energy of 5 MeV at 423 K to a fluence of 5×10^{18} cm^{-2} in pure helium. The irradiated and unirradiated specimens were isothermally annealed at 473 and 923 K.

RESULTS

The electron-microscopic examination of the microstructure of the alloys has shown that the average grain size in all of the alloys is 20–30 μm. Upon quenching from 1473 K and the irradiation by electrons at 423 K to a fluence of 5×10^{18} cm^{-2}, the density of dislocation loops in the N36 alloy is 4.2×10^{16} cm^{-3}, the loop size is ~8 nm, and the density of dislocations is ~5×10^{10} cm^{-2}.

The examination of the microstructure of the Fe–Ni–Al alloy has shown a tweed (ripple-like) contrast for all the specimens (both after quenching and after irradiation by electrons). This contrast can be clearly seen in the extinction contours. Upon quenching, dislocations are rare, and their density is 2×10^9 cm^{-2}. After irradiation by electrons, the density of dislocations somewhat increases, and stacking faults can be sometimes seen. Upon irradiation to a fluence of 5×10^{18} cm^{-2}, the density of dislocations is ~ 3×10^9 cm^{-2}. No precipitates of the secondary phase have been detected, possibly due to their small size and to their coherency with the matrix. After 5 h of thermal aging at 923 K, a ~8-nm secondary-phase precipitate of a Ni_3Al type has been found.

In the Fe–Ni–Ti alloy, the evolution of intermetallic-compound precipitates was additionally studied using STM. In the as-quenched alloy, hardly any precipitates was found. They have also not been detected after this alloy was annealed at a temperature equal to the irradiation temperature (423 K). After the irradiation of the alloy at 423 K, the formation and growth of the precipitates were observed. Figure 1 shows the dependence of the average size of the precipitates on the electron fluence. It can be seen that, with an increase in the irradiation dose, the growth in the precipitate size gradually decelerates. The size distribution of the precipitates after irradiation to the maximum dose of 5×10^{18} cm^{-2} has been obtained (Fig. 2). The average size of the secondary-phase precipitates is 4 nm. The density of the precipitates is ~2×10^{17} cm^{-3} and remains almost unchanged in the course of irradiation. This figure also shows the results of annealing (at a temperature of 473 K) the specimen irradiated at 423 K for a period comparable to the duration of irradiation. It can be seen that the distribution function hardly changed due to annealing. This indicates that,

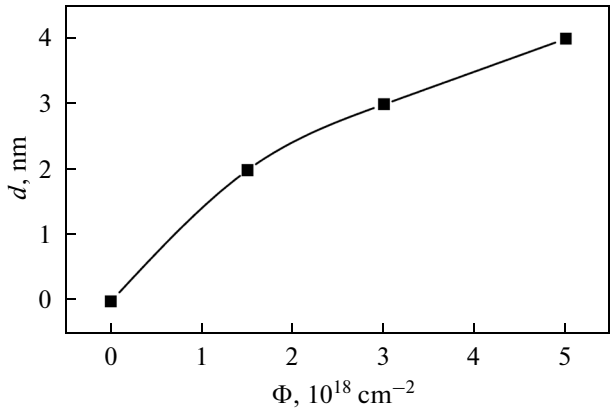

Fig. 1. Dependence of the average size of intermetallic-particle precipitates in the Fe–Ni–Ti alloy on the dose of electron irradiation at 423 K.

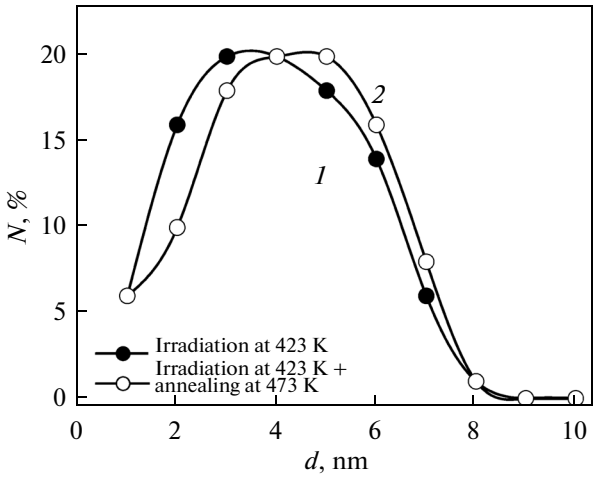

Fig. 2. Size distributions of intermetallic-compound particles after (*1*) electron irradiation at 423 K and (*2*) the same irradiation, followed by annealing at 473 K.

at the above-mentioned temperatures, no substantial activation of the thermal diffusion of Ti occurs.

The experimental data on the thermal aging of the as-quenched alloy show that the formation of the new phase begins at a temperature of ~550 K. The current–voltage characteristics (CVCs) were obtained for various portions of the specimen. At the characteristic sites, the CVCs were recorded at least at ten points. For comparison, in addition to CVCs for the irradiated specimens, they were also obtained for the unirradiated as-quenched specimen (the matrix) and for the Ni_3Ti specimen. At sites of nanosized precipitates, the CVC for the irradiated specimen is similar to that for the Ni_3Ti specimen and substantially differs from that for the matrix. This allows us to assume that the nanosized precipitations resulted from the irradiation have the composition Ni_3Ti. This conclusion agrees with the electron-microscopic data [10]. Figure 3 shows the dependences of the residual electric resistivity of the alloys on the electron fluence obtained at 423 K. It can be seen that the residual electric resistivity increases with increasing electron fluence. The increment in the residual electric resistivity in the Fe–Ni alloy is substantially greater than that in Fe–Ni–Al and Fe–Ni–Ti alloys.

It is known that the residual electric resistivity in these alloys is sensitive both to the phase separation of the solid solution and to the formation of secondary-phase precipitates [11]. The increase in the electric resistivity of the Fe–Ni–Al and Fe–Ni–Ti alloys (due to the irradiation and the irradiation, followed by the annealing) at the used exposure doses is caused by the decomposition of the solid solution, i.e., by the formation and growth of the precipitates of the intermetallic γ' phase (see Figs. 1, 2). In the Fe–Ni alloy, the phase separation of the solid solution occurs.

Figure 4 shows the results of measuring the coefficient of thermal expansion (CTE) of the alloys at a temperature of ~320 K after the electron irradiation, which indicate an increase in the CTE of all the alloys due to the irradiation. For the Fe–Ni alloy, an increase in the CTE indicates the occurrence of the processes of phase separation, as was shown in [5]. For the Fe–Ni–Al and Fe–Ni–Ti alloys, the initial CTE is substantially higher than that for the Fe–Ni alloy, since this takes place after irradiation. The Fe–Ni–Al and Fe–Ni–Ti alloys exhibit similar behaviors in the course of the irradiation. An increase in their CTEs is due to the formation of secondary-phase precipitates.

Figure 5 shows the dependences of the mechanical characteristics of the Fe–Ni, Fe–Ni–Al, and Fe–Ni–Ti alloys on the irradiation dose. It can be seen that at the initial stage of the irradiation radiation-induced strengthening occurs. With a further increase in the irradiation dose (to 1.5×10^{18} cm^{-2}), the yield stress decreases, unlike the Fe–Ni alloy. Similar

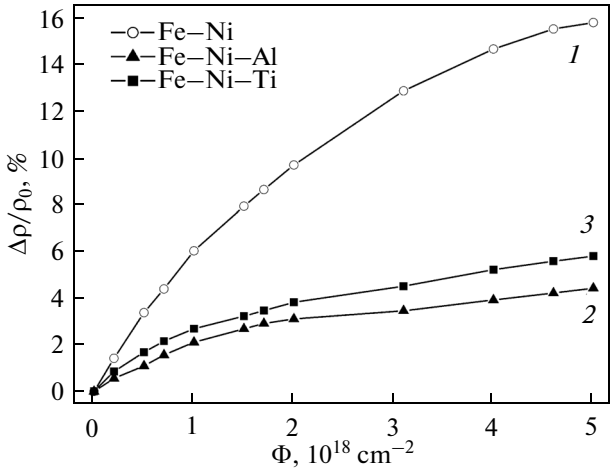

Fig. 3. Dose dependences of the increment in the residual electric resistivity for (*1*) Fe–Ni, (*2*) Fe–Ni–Al, and (*3*) Fe–Ni–Ti alloys.

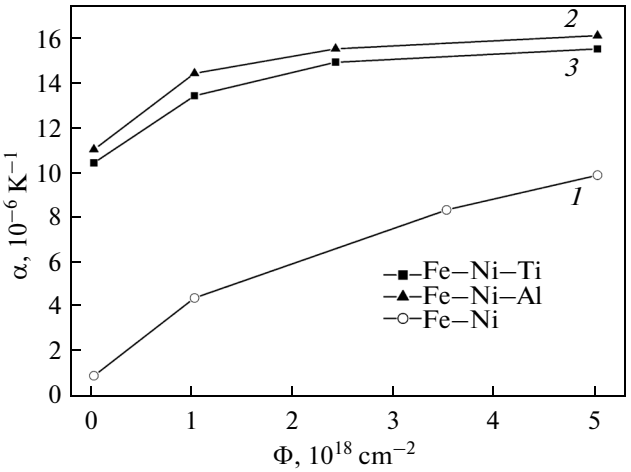

Fig. 4. Dose dependences of the linear coefficient of thermal expansion for (*1*) Fe–Ni, (*2*) Fe–Ni–Al, and (*3*) Fe–Ni–Ti alloys.

dependences are obtained for the ultimate strength. The ductility of the Fe–Ni alloy initially decreases; then, at a dose of over 1.5×10^{18} cm^{-2}, it remains almost unchanged. The ductility of the Fe–Ni–Al and Fe–Ni–Ti alloys changes only slightly; with an increase in the irradiation dose, the ductility tends to decrease.

DISCUSSION

It is known that, in modified alloys, solid-solution hardening (with no new phases appeared) occurs due to the blockage of dislocations by impurity atoms [13]. In our case, the higher yield stress and ultimate strength, as well as a lower ultimate elongation, for the quenched Fe–Ni–Al and Fe–Ni–Ti alloys compared to those for the Fe–Ni alloy are apparently related only to the solid-solution hardening because of the presence of Ti and Al in the solid solution. In the case of the solid-solution hardening, an increase in the yield stress $\Delta\sigma_{02}^{s}$ is described by the following expression [13]:

$$\Delta\sigma_{02}^{s} = ZG\varepsilon^{3/2}c^{1/2}, \quad (1)$$

where $Z = 1/760$; G is the shear modulus; ε is the discrepancy parameter related to the difference in the lattice parameters of atoms of the dissolved elements and the matrix, as well as in the moduli of elasticity of these elements and the matrix; and c is the concentration of atoms of the dissolved elements.

As was shown above, in the Fe–Ni–Al and Fe–Ni–Ti alloys the alloying elements are present in the solid solution. Assuming that, with varying concentration of an alloying element, the coefficients in expression (1) remain unchanged, we estimate the increment in the yield stress for the Fe–Ni–Al and Fe–Ni–Ti alloys relative to the yield stress of the

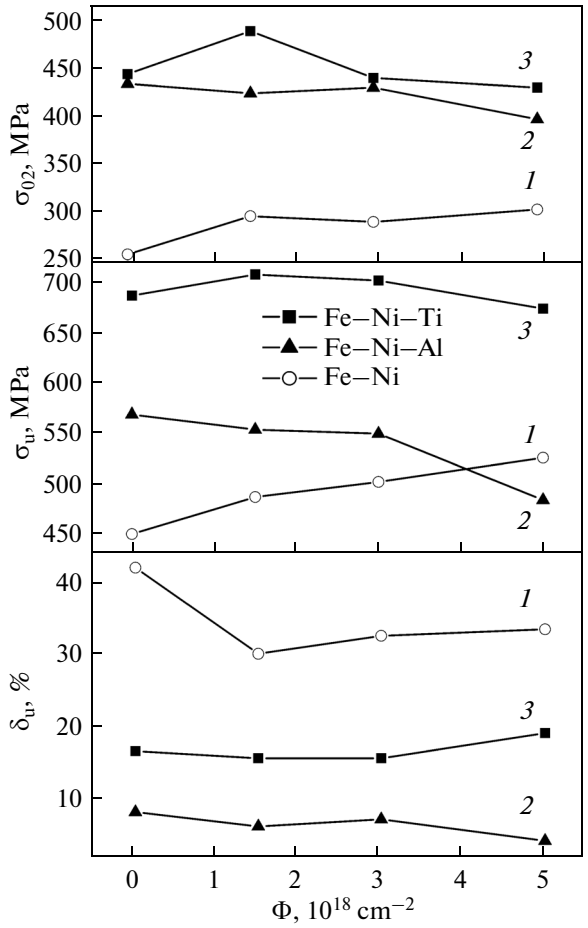

Fig. 5. Dependences of the yield stress, ultimate strength, and relative elongation for (*1*) Fe–Ni, (*2*) Fe–Ni–Al, and (*3*) Fe–Ni–Ti alloys on the dose of electron irradiation at 423 K.

Fe–Ni alloy at 178 and 188 MPa, respectively. Taking into account the difference in the concentrations of the alloying elements, we obtain that the predicted increment in the yield stress per 1 at % of the concentration of an alloying element is 109 MPa for Ti and 54 MPa for Al. Thus, the solid-solution hardening in the case of alloying with titanium is almost twice as efficient as in the case of alloying with aluminum.

Let us discuss the possible mechanisms of radiation-induced strengthening in the Fe–Ni alloy. As was shown above, in the course of irradiation, two processes occur in this alloy, i.e., the phase separation of the solid solution and the accumulation of vacancy clusters (VCs). It is known that the increment in the yield stress during irradiation related to VCs can be written as follows [14]:

$$\Delta\sigma_{02}(\text{VCs}) = \frac{2F}{b}\sqrt{d_i c_i}, \quad (2)$$

where F is the force that should be applied to a dislocation for overcoming an obstacle; b is the Burgers vector; and c_i and d_i are the density and size of obsta-

cles, respectively, assuming that all obstacles are of the same size. Otherwise, it would be necessary to take into account the size distribution of the obstacles. There are grounds to believe that, in our case, the size distribution of VCs is much narrower than in the case of neutron irradiation that produces cascades of atomic displacements.

The data on the annihilation of positrons show that, upon electron irradiation at a temperature of 423 K, the accumulation of VCs is observed; at doses of over $(2–3) \times 10^{18}$ cm^{-2}, the concentration of these VCs reaches a quasistationary level. This accumulation of the VCs is observed in the Fe–Ni alloy, as well as in the Fe–Ni–Al and Fe–Ni–Ti alloys [8, 11].

It can be believed that the phase separation of the solid solution in the Fe–Ni alloy increases the yield stress. However, the contribution of this phase separation has not been yet determined and additional studies are called for revealing its role. At a dose of 5×10^{18} cm^{-2}, the total contribution from these processes to the increment of the yield stress of the Fe–Ni alloy is 47 MPa. In the Fe–Ni–Al and Fe–Ni–Ti alloys, the contribution from the VCs to the increase in the yield stress cannot exceed this value.

Let us now discuss the mechanical characteristics of the irradiated Fe–Ni–Al and Fe–Ni–Ti alloys. The following three factors determine changes in the mechanical characteristics of these alloys:

(1) solid-solution hardening;

(2) the radiation-induced formation of intermetallic precipitates (with account for their evolution);

(3) the accumulation of radiation-induced defects (VCs).

It is generally thought that the yield stress is the sum of the contributions from each mechanism of strengthening. Proceeding from this and taking into account the estimates, we can assert that the two last factors should increase the yield stress. However, our experiments have shown a decrease in the yield stress with increasing irradiation dose. The most reasonable explanation of this fact is the assumption on the relief of the solid-solution hardening during irradiation due to a decrease in the concentration of titanium or aluminum in the solid solution.

If it is assumed that the decrease in the yield stress results from the relief of the solid-solution hardening due to the formation of intermetallic-compound precipitates, then, using expression (1) and the experimental data on the yield stress, the amount of titanium removed from the solid solution of the Fe–Ni–Ti alloy can be assumed to be ~0.4 at %. This estimate seems fairly reasonable.

The hardening related to the formation of the intermetallic-compound precipitates depends on their size and concentration. As was shown above, in the course of irradiation, the density of the intermetallic-compound precipitates remains almost unchanged; only the growth of the precipitates occurs. It is known that the maximum hardening is observed at a definite combination of the size and density of the precipitates. It can be seen in Fig. 5 that, in the Fe–Ni–Ti alloy the maximum hardening is achieved at a dose of $(1.5–2.0) \times 10^{18}$ cm^{-2}. Figure 1 shows that at this dose the precipitate size is 2.0–2.5 nm.

The analysis of the obtained results allows us to draw the conclusion that in the Fe–Ni alloy vacancy clusters play the leading role in radiation-induced strengthening, while in the Fe–Ni–Al and Fe–Ni–Ti alloys a substantial role is played by the evolution of the secondary-phase precipitations and the relief of the solid-solution hardening, in addition to the vacancy clusters.

ACKNOWLEDGMENTS

This work was supported in part by the Ural Branch of the Russian Academy of Sciences (project no. 12-M-23-2031m) an in part by the Russian Foundation for Basic Research (projects nos. 11-03-00018 and 14-03-00359).

REFERENCES

1. V. L. Arbuzov, B. N. Goshchitskii, S. E. Danilov, Yu. N. Zuev, A. E. Kar'kin, and V. V. Sagaradze, "Radiation defects and hydrogen in austenitic and austenitic–martensitic steels under low-temperature neutron irradiation," Phys. Met. Metallogr. **109**, 300–308 (2010).
2. S. N. Votinov, V. I. Prokhorov, and Z. E. Ostrovskii, *Irradiation of Stainless Steel* (Nauka, Moscow, 1987) [in Russian].
3. V. F. Zelenskii, I. M. Neklyudov, L. S. Ozhigov, et al., *Some Problems of Physics of Material Radiation Damages* (Naukova Dumka, Kiev, 1979) [in Russian].
4. V. L. Arbuzov, B. N. Goshchitskii, S. E. Danilov, A. V. Kar'kin, and D. A. Perminov, "Effect of neutron and electron irradiation on radiation-induced separation of solid solutions in the Fe–Ni and Fe–Ni–P alloys," Phys. Met. Metallogr. **106**, 266–275 (2008).
5. S. E. Danilov, V. L. Arbuzov, and V. A. Kazantsev, "Radiation-induced separation of solid solution in Fe–Ni invar," J. Nucl. Mater. **414**, 200–204 (2011).
6. V. V. Sagaradze, B. N. Goshchitskii, and V. L. Arbuzov, "Dispersion-strengthened austenite steel for fast-neutron reactors," Vopr. At. Nauki Tekhn., Ser. Materialoved. Nov. Mater., No. 1, 258–266 (2005).
7. F. A. Garner, "Void swelling and irradiation creep in light water reactor environments," Understanding and Mitigating Ageing in Nuclear Power Plants, No. 4, 308–356 (2010).
8. D. A. Perminov, A. P. Druzhkov, and V. L. Arbuzov, "Role of intermetallic nanoparticles in radiation damage of austenitic Fe–Ni–based alloys studied by

positron annihilation," J. Nucl. Mater. **414**, 186–193 (2011).

9. A. P. Druzhkov, V. L. Arbuzov, and D. A. Perminov, "Positron annihilation study of effects of Ti and plastic deformation on defect accumulation and annealing in electron-irradiated austenitic steels and alloys," J. Nucl. Mater. **341**, 153–163 (2005).
10. V. L. Arbuzov, K. V. Shal'nov, S. E. Danilov, A. E. Davletshin, N. L. Pecherkina, and V. V. Sagaradze, "Observation of segregation deposits in iron–nickel–titanium alloy using scanning tunneling microscopy", Techn. Phys. Lett. **25**, 134–135 (1999).
11. S. E. Danilov, V. L. Arbuzov, A. P. Druzhkov, and K. V. Shal'nov, "Annealing of radiation defects in N36 alloys alloyed by phosphorus and titanium", Vopr. At. Nauki Tekhn., Ser. FRP I PM, No. 4, 3–6 (2000).
12. F. Duffaut and R. Cozar, "Property adjustments in controlled expansion and elasticity alloys, in *The Iron–Nickel Alloys* (Lavoisier, 2003), pp. 109–139.
13. *Physics of Solid State. Encyclopedic Dictionary*, Ed. by V. G. Bar'yakhtar (Naukova Dumka, Kiev, 1998), Vol. 2 [in Russian].
14. Sh. Sh. Ibragimov and V. V. Kirsanov, "Radiation strengthening of metals," in *Radiation Defects in Metallic Crystals* (Nauka, KazSSR, Alma-Ata, 1978), pp. 64–77 [in Russian].

Translated by D. Tkachuk